Available online at www.sciencedirect.com
SCIENCE DIRECT®
Vacuum 76 (2004) 73–81
VACUUM
SURFACE ENGINEERING, SURFACE INSTRUMENTATION & VACUUM TECHNOLOGY
www.elsevier.com/locate/vacuum

Isothermal slip flow over curved surfaces ☆

R.W. Barber*, Y. Sun, X.J. Gu, D.R. Emerson

Centre for Microfluidics, CCLRC Daresbury Laboratory, Warrington, WA4 4AD, UK

Received 6 May 2004; accepted 17 May 2004

Abstract

It has long been recognised that the no-slip-boundary condition employed in the Navier–Stokes equations can only be applied when the Knudsen number, $Kn \leqslant 10^{-3}$. If the Knudsen number is increased beyond this value, rarefaction effects start to influence the flow and the molecular collision frequency per unit area becomes too small to maintain the no-slip-boundary condition. Unfortunately, Maxwell's famous slip equation describing the velocity discontinuity at the wall is often misapplied when analysing flows over curved or rotating boundaries. In the present study, a generalised version of Maxwell's slip equation is used to investigate low Knudsen number isothermal flow over walls with substantial curvature. The generalised slip equation is written in terms of the tangential shear stress to overcome the limitations of the conventional slip-boundary treatment. The study considers a number of fundamental, but challenging, rarefied flow problems and demonstrates that Maxwell's conventional slip equation is unable to capture important flow phenomena over curved or rotating surfaces.

Keywords: Slip flow; Knudsen number; Rarefied gas dynamics; Non-continuum; Navier–Stokes equations

1. Introduction

Non-continuum or rarefied gas flows are encountered in both low-pressure/vacuum applications [1–3], as well as in micron-sized devices which operate at standard atmospheric conditions [4,5]. Historically, many of the pioneering investigations of non-continuum flows were conducted by researchers in the rarefied gas community who were primarily interested in low-pressure applications [6–9]. However, the emergence of micro-electro-mechanical-systems (MEMS) and the associated advances in micro-machining technology have enabled fluidic devices to be constructed with feature sizes down to 1 μm, leading to a range of new applications where rarefaction effects need to be considered. As an example, recent experiments on silicon micro-fluidic channels have confirmed that conventional (continuum) flow analyses are unable to predict the observed mass flow rates through micron-sized devices with any degree of accuracy [10–16]. This has resulted in the growing

☆ Based on a paper presented at the Spanish Vacuum Society Workshop on Gas Dynamics, Avila, 30 June–2 July 2003.

*Corresponding author. Tel.: +44-1925-603221; fax: +44-1925-603634.

E-mail address: r.w.barber@dl.ac.uk (R.W. Barber).

0042-207X/$ - see front matter © 2004 Elsevier Ltd. All rights reserved.
doi:10.1016/j.vacuum.2004.05.012

realisation that the fluid mechanics at micron and sub-micron scales is significantly different from the macroscopic world and has many similarities with vacuum gas dynamics.

The continuum assumption in the Navier–Stokes equations is only valid when the mean free path of the gas molecules is smaller than the characteristic dimension of the flow domain. If this condition is violated, the fluid will no longer be in local thermodynamic equilibrium and a variety of rarefaction effects will be exhibited, including the presence of slip between the gas and the substrate. Velocity profiles, boundary wall shear stresses and mass flow rates will then be influenced by the non-continuum flow regime. In addition, there is significant experimental evidence to suggest that the gas–surface interactions at the wall are affected by incomplete momentum accommodation [14–18].

The fundamental difficulty in predicting gas transport within conventional vacuum environments and micro-fluidic devices can be attributed to the breakdown of the continuum assumption in the Navier–Stokes equations. The degree of rarefaction of a gas (and the applicability of the Navier–Stokes equations) is determined by the Knudsen number, Kn, which is defined as the ratio of the mean free path of the gas molecules, λ, to the characteristic dimension of the flow geometry, L

$$Kn = \frac{\lambda}{L}. \tag{1}$$

The most appropriate method of flow analysis depends crucially on the degree of rarefaction within the gas. Schaaf and Chambre [19] proposed the following classification system based upon the magnitude of the local Knudsen number. For $Kn \leqslant 10^{-2}$, the continuum hypothesis is appropriate and the flow can be described by the Navier–Stokes equations using conventional no-slip-boundary conditions, although Gad-el-Hak [20] has suggested that the breakdown in the continuum assumption is discernible at Knudsen numbers as low as $Kn = 10^{-3}$. For $Kn > 10$, the continuum approach breaks down completely and the regime can then be described as being a *free molecular flow*. Under such conditions, the mean free path of the molecules is far greater than the characteristic length scale and consequently molecules reflected from a solid surface travel, on average, many lengths scales before colliding with other molecules. However, for Knudsen numbers between $Kn = 10^{-2}$ and 10, the fluid can neither be considered an absolutely continuous medium nor a free molecular flow. In the range, $10^{-2} \leqslant Kn \leqslant 10^{-1}$ (commonly referred to as the *slip-flow* regime), the Navier–Stokes equations are considered to offer a reasonable description of the flow provided tangential slip-velocity boundary conditions are implemented between the gas and the substrate. On the other hand, for $10^{-1} \leqslant Kn \leqslant 10$ (*transition flow*), the Navier–Stokes constitutive equations and first-order slip-boundary conditions begin to break down and alternative methods of analysis must be considered. The application of continuum-based flow models for the transition regime is an active research area and has resulted in the Burnett [21], Bhatnagar-Gross-Krook (BGK)-Burnett [22], Grad's [23] and Woods' [24] equations. These higher-order continuum models require correspondingly higher-order slip-boundary conditions. Alternatively, proper theoretical treatment of the entire Knudsen flow regime ($0 < Kn < \infty$) can be achieved by solving the Boltzmann transport equation [25], but the method is fraught with difficulties in calculating the collision integral terms. A practical alternative to solving the Boltzmann equation is the direct simulation Monte Carlo (DSMC) approach proposed by Bird [26]. While the use of particle-based techniques is eminently suitable for transition and free molecular studies, the DSMC approach requires large numbers of particles for accurate simulation in the slip-flow regime, making the technique prohibitively expensive in terms of computational time and memory requirements. As pointed out by Agarwal et al. [27], the computing requirements of many DSMC simulations in two- and three-dimensions for $Kn \approx O(1)$, are still beyond the limits of available computing power. It is therefore apparent that continuum-based models represent the most appropriate method of analysis for the near-continuum and slip-flow regimes.

Several studies have attempted to increase the accuracy of slip-flow predictions by proposing higher-order boundary conditions [28–34]. The use of higher-order slip conditions with the Navier–Stokes constitutive equations can be justified because rarefied flows are dominated by gas–surface interactions at the wall, and therefore adopting a more accurate model at the boundary will have a significant effect on the overall accuracy of the predictions. Unfortunately, many slip-flow models overlook the fact that the conventional form of Maxwell's first-order boundary treatment is only applicable to planar surfaces. For simulations involving curved or moving surfaces, this means that important physics of the gas–surface interactions can be lost.

The present investigation considers low Knudsen number isothermal flows over curved surfaces and demonstrates that the conventional form of Maxwell's slip equation suffers considerable loss in accuracy when applied to non-planar boundaries. A particularly important aspect of the present study is the proper formulation of the first-order slip-velocity boundary condition so that it can be applied to a generalised curved surface. This is accomplished by recasting Maxwell's slip equation as a function of the local wall shear stress. The resulting generalised boundary condition is shown to provide an improved description of curved slip flow and, more importantly, does not suffer from some of the limitations of the conventional slip-boundary treatment. It is envisaged that a similar technique could also be used to provide a generalised higher-order slip-boundary condition. This could be achieved by replacing the shear stress defined in the Navier–Stokes equations by a higher-order stress tensor from, for example, the Burnett equations. Unlike existing second-order boundary conditions which are only applicable to planar walls, the resulting boundary condition would be directly applicable to three-dimensional flows over curved and rotating surfaces.

2. Governing hydrodynamic equations

The Navier–Stokes equations governing the flow of a continuous (infinitely divisible) fluid can be written in tensor notation as follows:

$$\textit{continuity}: \quad \frac{\partial \rho}{\partial t} + \frac{\partial(\rho u_k)}{\partial x_k} = 0 \tag{2}$$

and

$$\textit{momentum}: \quad \frac{\partial(\rho u_i)}{\partial t} + \frac{\partial(\rho u_k u_i)}{\partial x_k} = -\frac{\partial p}{\partial x_i} + \frac{\partial \tau_{ik}}{\partial x_k}, \tag{3}$$

where u is the velocity, p is the pressure, ρ is the fluid density and τ_{ik} is the second-order stress tensor. For a Newtonian, isotropic fluid, the stress tensor is given by

$$\tau_{ik} = \mu_1 \left(\frac{\partial u_i}{\partial x_k} + \frac{\partial u_k}{\partial x_i} \right) + \mu_2 \left(\frac{\partial u_j}{\partial x_j} \right) \delta_{ik}, \tag{4}$$

where μ_1 and μ_2 are the first and second coefficients of viscosity, respectively, and δ_{ik} is the unit second-order tensor (Kronecker delta). The second coefficient of viscosity can be eliminated from the Navier–Stokes equations by means of Stokes' continuum hypothesis:

$$\mu_2 + \tfrac{2}{3}\mu_1 = 0 \tag{5}$$

although the validity of the above assumption has occasionally been questioned for fluids other than dilute monatomic gases [35].

2.1. Slip-flow-boundary conditions

In traditional (continuum) flow analyses, a no-slip velocity constraint is enforced along all solid walls. In practice, the no-slip condition is found to be appropriate when the Knudsen number, $Kn \leqslant 10^{-3}$. If the Knudsen number is increased beyond this value, rarefaction effects start to influence the flow and the molecular collision frequency per unit area becomes too small to ensure local thermodynamic equilibrium and the no-slip-boundary condition begins to break down. Under these conditions, a discontinuity will occur in the velocity at the wall and the gas will effectively slide over the solid surface. The discontinuity in the velocity can be described using Maxwell's famous slip-velocity equation [36]

$$u_{\text{slip}} = \frac{(2-\sigma)}{\sigma} \lambda \left. \frac{\partial u}{\partial y} \right|_{y=0}, \tag{6}$$

where u_{slip} is the tangential slip-velocity at the wall ($y=0$), u is the tangential velocity component, y is the distance normal to the wall, λ is the mean free path of the gas and σ is the Tangential Momentum Accommodation Coefficient (TMAC). The TMAC accounts for the average streamwise (or tangential) momentum exchange between the molecules and the solid surface and can vary from zero (for specular reflection) up to unity (for complete or diffuse accommodation).

Eq. (6) is normally remembered as Maxwell's slip-velocity boundary condition but closer scrutiny of the derivation indicates that the equation should only be applied to planar surfaces. As a consequence, Maxwell's boundary condition is commonly misapplied in practical situations involving surface curvature. Maxwell [36] initially derived the slip-boundary condition in terms of the viscous shear stress (Eq. (66), p. 253) but then simplified the resulting expression, presumably believing that the variation in wall-normal velocity could be neglected. Maxwell's use of a one-dimensional expression for the shear stress (appropriate for the problem being analysed) made his result only valid for planar, non-rotating walls. However, if the viscous shear stress is retained in the derivation then the generalised version of Maxwell's slip-velocity boundary condition can be written as

$$u_{slip} = \frac{(2-\sigma)}{\sigma}\frac{\lambda}{\mu}\tau_t|_{y=0}, \tag{7}$$

where $\tau_t|_{y=0}$ is the tangential shear stress at the wall. In the case of a two-dimensional surface, Eq. (7) can be rewritten as

$$u_{slip} = \frac{(2-\sigma)}{\sigma}\lambda\left(\frac{\partial u}{\partial y}+\frac{\partial v}{\partial x}\right)\Big|_{y=0}, \tag{8}$$

where u_{slip} is the tangential slip-velocity at the wall ($y=0$) and (u,v) are the velocity components of the gas, tangential and normal to the wall, respectively. The additional velocity derivative in Eq. (8) compared with Eq. (6) can have a significant influence on the overall slip-flow behaviour. For example, in flow problems that include surface curvature, the application of Eq. (6) is totally inappropriate since the boundary condition fails to account for the fact that the velocity normal to the wall can vary in the streamwise direction. Simulations involving Eq. (6) are therefore likely to lose important physics of the gas–surface interactions at curved walls, leading to incorrect slip-flow behaviour.

Although the misapplication of Maxwell's conventional slip-velocity boundary condition, Eq. (6), is widespread, there are several instances where curved boundaries have been treated correctly [37–40]. For example, as early as 1888, Basset [37] analysed creeping flow past a sphere and correctly accounted for surface curvature in his slip equation. Other researchers recognising the importance of accounting for the curved wall include Wang [38] who analysed Stokes' slip flow through a regular grid of circular cylinders and Aoki et al. [39] who investigated rarefied Couette flow between two co-axial cylinders. In addition, Einzel et al. [40] have developed a similar boundary condition to Eq. (7) based upon the concept of slip length.

Unfortunately, there are numerous studies that implement the conventional form of Maxwell's slip condition over curved or moving surfaces. To illustrate the importance of implementing the generalised slip equation, we present two examples that demonstrate the limitations of the conventional boundary treatment.

3. Low Knudsen number Couette flow between two co-axial cylinders

Cylindrical Couette flow in the continuum regime is a classical problem that can be found in many fluid dynamics textbooks. However, recent analytical and DSMC studies [39–41] have suggested that under certain conditions of rarefaction (in particular, when the accommodation coefficient is small), the velocity profile between the cylinders reverses direction so that the gas moves faster near the stationary outer cylinder. This anomalous behaviour has been described as an 'inverted velocity profile' because the velocity of the gas increases with distance from the rotating inner cylinder. The effect is completely non-intuitive and contrary to the normal velocity profile expected within a cylindrical Couette flow.

The present investigation considers an inner cylinder of radius, R_1, rotating at a constant angular velocity, ω, and a stationary outer cylinder of radius, R_2. Both cylinders are maintained at the same temperature and therefore the flow is considered to be isothermal. The Navier–Stokes equations can be solved analytically by integrating the tangential momentum conservation equation across the annular ring and imposing the appropriate slip-boundary conditions at the inner and outer radii. For a polar co-ordinate (r,θ) reference frame, the generalised form of Maxwell's slip-boundary equation at the inner rotating cylinder can be written as

$$u_\theta|_{r=R_1} = \omega R_1 + \frac{(2-\sigma)}{\sigma}\,\lambda\left(\frac{\partial u_\theta}{\partial r} - \frac{u_\theta}{r}\right)\bigg|_{r=R_1} \tag{9}$$

while the generalised slip-boundary condition at the stationary outer cylinder can be written as

$$u_\theta|_{r=R_2} = -\frac{(2-\sigma)}{\sigma}\,\lambda\left(\frac{\partial u_\theta}{\partial r} - \frac{u_\theta}{r}\right)\bigg|_{r=R_2}. \tag{10}$$

Following the notation adopted by Einzel et al. [40], the tangential velocity profile can be shown to be defined by

$$u_\theta(r) = \frac{\omega}{A-B}\left(Ar - \frac{1}{r}\right), \tag{11}$$

where

$$A = \frac{1}{R_2^2}\left(1 - 2\,\frac{\zeta_0}{R_2}\right); \quad B = \frac{1}{R_1^2}\left(1 + 2\,\frac{\zeta_0}{R_1}\right) \tag{12}$$

and the slip length, ζ_0, is given by

$$\zeta_0 = \frac{(2-\sigma)}{\sigma}\,\lambda. \tag{13}$$

If the analysis is repeated using the conventional (incorrect) slip-boundary condition presented in Eq. (6), the gas velocities at the inner and outer radii are given by

$$u_\theta|_{r=R_1} = \omega R_1 + \frac{(2-\sigma)}{\sigma}\,\lambda\,\frac{\partial u_\theta}{\partial r}\bigg|_{r=R_1} \tag{14}$$

and

$$u_\theta|_{r=R_2} = -\frac{(2-\sigma)}{\sigma}\,\lambda\,\frac{\partial u_\theta}{\partial r}\bigg|_{r=R_2}. \tag{15}$$

It can be shown that the tangential velocity profile then becomes

$$u_\theta(r) = \frac{\omega}{A-B}\left(\frac{R_1}{R_1-\zeta_0}\right)\left(Ar - \frac{1}{r}\right), \tag{16}$$

where

$$A = \frac{1}{R_2^2}\left(\frac{R_2-\zeta_0}{R_2+\zeta_0}\right) \quad \text{and} \quad B = \frac{1}{R_1^2}\left(\frac{R_1+\zeta_0}{R_1-\zeta_0}\right). \tag{17}$$

As an aside, in the limiting condition of $\lambda \to 0$, Eqs. (11) and (16) both tend to the continuum solution for cylindrical Couette flow:

$$u_\theta(r) = \frac{\omega R_1^2 R_2^2}{(R_1^2 - R_2^2)}\left(\frac{1}{R_2^2}\,r - \frac{1}{r}\right). \tag{18}$$

For compatibility with DSMC data presented by Tibbs et al. [41], the inner and outer cylinders are chosen to have radii of 3λ and 5λ, respectively, and the tangential momentum accommodation coefficient, σ, is chosen to be 0.1. Fig. 1 shows a comparison of the velocity profiles (non-dimensionalised by the tangential velocity of the inner cylinder) predicted using the standard no-slip-boundary condition, the conventional slip condition, the generalised slip condition and DSMC (direct simulation Monte Carlo) simulations [41]. The DSMC results can be regarded as an independent numerical test in the absence of

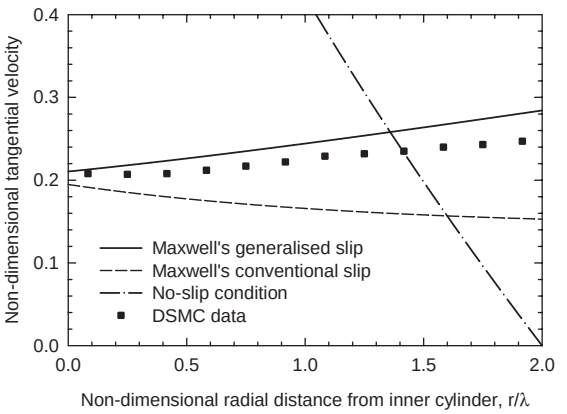

Fig. 1. Non-dimensionalised velocity profiles for a cylindrical Couette flow. Comparison of no-slip condition, Maxwell's conventional slip condition (Eq. (6)), Maxwell's generalised slip condition (Eq. (7)) and DSMC data [41].

definitive experimental data. The fact that DSMC simulations predict an inverted velocity profile (with the gas travelling faster near the stationary outer wall) is strong evidence to suggest the phenomenon exists. The flow has also been studied by Aoki et al. [39] using two alternative formulations: a systematic asymptotic analytical solution for small Knudsen numbers, and a direct numerical solution of the Boltzmann equation using the BGK approximation [42]. The results again confirm the existence of an inverted velocity profile for small values of accommodation coefficient.

Inspection of Fig. 1 shows that the analytical solution using the conventional slip-boundary condition cannot predict the velocity inversion and instead yields a velocity profile which decreases with distance from the rotating inner cylinder. On the other hand, the generalised slip-boundary condition is able to capture the important physics of the velocity inversion process. The quantitative agreement between the DSMC data and the analytical predictions is not particularly close but this is to be expected since the separation distance between the cylinder walls is only two mean free paths, implying a Knudsen number (based upon the annular clearance) of 0.5. At such a high Knudsen number, continuum-based flow models are likely to be at the limit of their applicability. Nevertheless, the results clearly highlight a potential problem with the conventional slip-velocity boundary condition.

4. Low Knudsen number isothermal flow past an unconfined sphere

Unconfined creeping flow past a sphere is another canonical fluid dynamics problem. The analysis was first performed for the continuum regime by Stokes [43] who demonstrated that in the absence of inertial forces, the total drag force, D_T, on an unconfined sphere of radius a, in a flow stream of velocity U, can be written as

$$D_T = 6\pi\mu U a. \tag{19}$$

The extension of Stokes' analysis to slip flow past a sphere was first proposed by Basset [37]. Most notably, the effects of slip were incorporated into the analysis using a velocity boundary condition that accounted correctly for the surface curvature. Basset's analysis did not specifically consider a rarefied gas, and instead employed an arbitrary slip coefficient, β, which related the tangential slip velocity at the wall to the local shear stress

$$\tau_{wall} = \beta u_{slip}. \tag{20}$$

However, defining the slip coefficient as

$$\beta = \frac{\mu}{\left(\frac{(2-\sigma)}{\sigma}\lambda\right)} \tag{21}$$

allows Basset's analytical result to be applied to rarefied gas flows. It should be noted that substituting Eq. (21) into (20) re-establishes the generalised slip-velocity condition presented earlier in Eq. (7).

Basset's original analysis only provided an expression for the total drag force on the sphere:

$$D_T = 6\pi\mu U a \times \left(1 + 2\frac{(2-\sigma)}{\sigma}\frac{\lambda}{a}\right) \Big/ \left(1 + 3\frac{(2-\sigma)}{\sigma}\frac{\lambda}{a}\right). \tag{22}$$

Barber and Emerson [44], however, have repeated Basset's analysis to predict the individual components of the drag force. In continuum (no-slip) flows, the normal stress must vanish along any rigid no-slip impermeable boundary [45]. In contrast, the tangential slip-boundary condition associated with rarefied flows generates a normal stress term which causes an additional force on the sphere. The total drag force is therefore composed of three separate components, namely skin friction drag (D_S), normal stress drag (D_N) and pressure (or form) drag (D_P). The analytical expressions for the individual drag components are presented in Table 1.

An important aspect of the present study is the proper treatment of the slip-boundary condition around curved surfaces. It is therefore interesting to consider the effects of utilising the conventional (incorrect) form of slip-boundary condition. If the analytical derivation is repeated using Eq. (6) instead of the correct slip velocity formulation, Eq. (7), then the total drag force on the sphere can

Table 1
Individual drag force components on an unconfined sphere in the slip flow regime

Drag component	Generalised slip-boundary condition, Eq. (7)	Conventional slip-boundary condition, Eq. (6)
Skin friction drag, D_S	$D_S = 4\pi\mu Ua \dfrac{1}{\left(1+3\frac{(2-\sigma)}{\sigma}\frac{\lambda}{a}\right)}$	$D_S = 4\pi\mu Ua \dfrac{\left(1-\frac{(2-\sigma)}{\sigma}\frac{\lambda}{a}\right)}{\left(1+2\frac{(2-\sigma)}{\sigma}\frac{\lambda}{a}\right)}$
Normal stress drag, D_N	$D_N = 4\pi\mu Ua \dfrac{\left(2\frac{(2-\sigma)}{\sigma}\frac{\lambda}{a}\right)}{\left(1+3\frac{(2-\sigma)}{\sigma}\frac{\lambda}{a}\right)}$	$D_N = 4\pi\mu Ua \dfrac{\left(2\frac{(2-\sigma)}{\sigma}\frac{\lambda}{a}\right)}{\left(1+2\frac{(2-\sigma)}{\sigma}\frac{\lambda}{a}\right)}$
Pressure drag, D_P	$D_P = 2\pi\mu Ua \dfrac{\left(1+2\frac{(2-\sigma)}{\sigma}\frac{\lambda}{a}\right)}{\left(1+3\frac{(2-\sigma)}{\sigma}\frac{\lambda}{a}\right)}$	$D_P = 2\pi\mu Ua \dfrac{\left(1+\frac{(2-\sigma)}{\sigma}\frac{\lambda}{a}\right)}{\left(1+2\frac{(2-\sigma)}{\sigma}\frac{\lambda}{a}\right)}$
Total drag, D_T	$D_T = 6\pi\mu Ua \dfrac{\left(1+2\frac{(2-\sigma)}{\sigma}\frac{\lambda}{a}\right)}{\left(1+3\frac{(2-\sigma)}{\sigma}\frac{\lambda}{a}\right)}$	$D_T = 6\pi\mu Ua \dfrac{\left(1+\frac{(2-\sigma)}{\sigma}\frac{\lambda}{a}\right)}{\left(1+2\frac{(2-\sigma)}{\sigma}\frac{\lambda}{a}\right)}$

be shown to be given by

$$D_T = 6\pi\mu Ua \times \left(1+\frac{(2-\sigma)}{\sigma}\frac{\lambda}{a}\right)\Big/\left(1+2\frac{(2-\sigma)}{\sigma}\frac{\lambda}{a}\right). \quad (23)$$

For completeness, Table 1 presents the individual drag force components arising from the incorrect boundary treatment.

Comparison of Eqs. (22) and (23) reveals that at the upper limit of the slip–flow regime, $Kn = \lambda/a = 10^{-1}$, the total drag force predicted by the two expressions differs by less than 1%, assuming complete momentum accommodation ($\sigma = 1$). However, in the limiting case of a perfectly smooth sphere such that all the incident molecules are reflected specularly ($\sigma = 0$), the conventional slip-boundary condition will underestimate the drag by 25%. It is also interesting to consider the variation in the skin friction drag component. In the limiting case of a perfectly smooth (specular) sphere, there is no mechanism by which the wall can transfer tangential momentum to or from the gas. Thus, the drag due to skin friction (D_S) must be zero for specular reflection. It can be seen that the drag predicted by the generalised boundary condition does indeed produce zero skin friction. On the other hand, the conventional slip condition gives a finite value of *negative* skin friction drag (i.e. a thrust). This non-physical prediction demonstrates the importance of employing

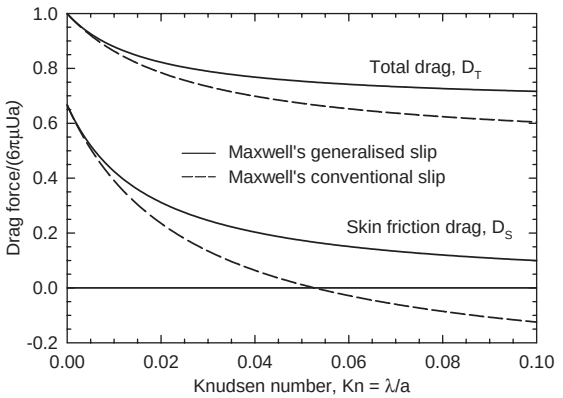

Fig. 2. Variation of total drag and skin friction drag on an unconfined sphere for $\sigma = 0.1$. Comparison of Maxwell's conventional slip condition (Eq. (6)) and Maxwell's generalised slip condition (Eq. (7)).

the generalised slip equation, as opposed to the conventional boundary treatment. The disparity between the analytical drag equations is illustrated in Fig. 2 for a tangential momentum accommodation coefficient of $\sigma = 0.1$. It can be seen that the exclusion of curvature effects in the conventional slip equation significantly alters the drag components on the sphere.

5. Conclusions

The present study considers a number of fundamental, but challenging, curved flow geometries and demonstrates that the conventional form of Maxwell's slip-boundary condition is unable to capture important physics over curved or rotating surfaces. For example, the conventional boundary equation is unable to predict an inverted velocity profile within a cylindrical Couette flow, and also fails to predict the correct asymptotic behaviour for specular flow ($\sigma = 0$) over an unconfined sphere.

A particularly important aspect of the present study is the proper formulation of the slip-boundary condition so that it can be applied to a generalised curved surface. This is accomplished by recasting Maxwell's slip-velocity equation as a function of the local wall shear stress. The resulting generalised equation does not suffer from the limitations of the conventional slip-boundary treatment and is shown to provide an improved description of curved slip flows.

Acknowledgements

This work was carried out as part of the μFAST program with support from the Medical Research Council under Grant reference 57719. Additional support was provided by the EPSRC under the auspices of Collaborative Computational Project 12 (CCP12).

References

[1] Muntz EP. Annual Rev Fluid Mech 1989;21:387–417.
[2] Tison SA. Vacuum 1993;44(11–12):1171–5.
[3] Livesey RG. J Vac Sci Technol A 2001;19(4):1674–8.
[4] Gabriel K, Jarvis J, Trimmer W. Small machines, large opportunities: a report on the emerging field of microdynamics. NSF Technical Report, 1988.
[5] Ho CM, Tai YC. Annual Rev Fluid Mech 1998;30:579–612.
[6] Brown GP, DiNardo A, Cheng GK, Sherwood TK. J Appl Phys 1946;17:802–13.
[7] Ebert WA, Sparrow EM. J Basic Eng 1965;87:1018–24.
[8] Sreekanth AK. Proceedings of the Sixth International Symposium on Rarefied Gas Dynamics. New York: Academic Press, 1968. p. 667–80.
[9] Porodnov BT, Suetin PE, Borisov SF, Akinshin VD. J Fluid Mech 1974;64:417–37.
[10] Pfahler J, Harley J, Bau H, Zemel JN. Micro-mech Sensors Actuators Systems 1991;32:49–60.
[11] Harley JC, Huang Y, Bau HH, Zemel JN. J Fluid Mech 1995;284:257–74.
[12] Arkilic EB, Breuer KS, Schmidt MA. Appl Microfabrication Fluid Mech 1994;197:57–66.
[13] Arkilic EB, Schmidt MA, Breuer KS. J Micro-Electro-Mech Systems 1997;6(2):167–78.
[14] Arkilic EB, Schmidt MA, Breuer KS. 20th International Symposium on Rarefied Gas Dynamics. Beijing University Press, 1997.
[15] Arkilic EB, Breuer KS, Schmidt MA. J Fluid Mech 2001;437:29–43.
[16] Maurer J, Tabeling P, Joseph P, Willaime H. Phys Fluids 2003;15(9):2613–21.
[17] Thomas LB, Lord RG. Eighth International Symposium on Rarefied Gas Dynamics. New York: Academic Press, 1974. p. 405–12.
[18] Seidl M, Steinheil E. Ninth International Symposium on Rarefied Gas Dynamics. DFVLR Press, 1974.
[19] Schaaf SA, Chambre PL. Flow of rarefied gases. Princeton: Princeton University Press; 1961.
[20] Gad-el-Hak M. J Fluids Eng 1999;121:5–33.
[21] Chapman S, Cowling TG. The mathematical theory of non-uniform gases: an account of the kinetic theory of viscosity, thermal conduction and diffusion in gases. Cambridge: Cambridge University Press; 1970.
[22] Balakrishnan R, Agarwal RK, Yun KY. J Thermophys Heat Transfer 1999;13(4):397–410.
[23] Grad H. Commun Pure Appl Math 1949;2:331–407.
[24] Woods LC. An introduction to the kinetic theory of gases and magnetoplasmas. Midsomer Norton: Oxford Science Publications; 1993.
[25] Sharipov F, Seleznev V. J Phys Chem Ref Data 1998;27(3):657–706.
[26] Bird G. Molecular gas dynamics and the direct simulation of gas flows. Oxford: Clarendon Press; 1994.
[27] Agarwal RK, Yun KY, Balakrishnan R. Phys Fluids 2001;13(10):3061–85.
[28] Deissler RG. Int J Heat Mass Transfer 1964;7:681–94.
[29] Hsia YT, Domoto GA. J Lubrication Tech 1983;105:120–30.

[30] Beskok A, Karniadakis GE. J Thermophys Heat Transfer 1994;8(4):647–55.
[31] Beskok A, Trimmer W, Karniadakis GE. J Fluids Eng 1996;118:448–56.
[32] Beskok A. Num Heat Transfer B 2001;40:451–71.
[33] Aubert C, Colin S. Microscale Thermophys Eng 2001;5: 41–54.
[34] Hadjiconstantinou NG. Phys Fluids 2003;15(8):2352–4.
[35] Gad-el-Hak M. J Fluids Eng 1995;117:3–5.
[36] Maxwell JC. Philos Trans Roy Soc Part 1 1879;170:231–56.
[37] Basset AB. A treatise on hydrodynamics. Cambridge: Cambridge University Press; 1888.
[38] Wang CY. Phys Fluids 2002;14(9):3358–60.
[39] Aoki K, Yoshida H, Nakanishi T, Garcia AL. Phys Rev E 2003;68:016302-1-11.
[40] Einzel D, Panzer P, Liu M. Phys Rev Lett 1990;64(19): 2269–72.
[41] Tibbs KW, Baras F, Garcia AL. Phys Rev E 1997;56(2): 2282–3.
[42] Bhatnagar PL, Gross EP, Krook M. Phys Rev 1954;94(3):511–25.
[43] Stokes GG. Cambridge Philos Trans 1851;9:8–106.
[44] Barber RW, Emerson DR. Analytical solution of low Reynolds number slip flow past a sphere. CLRC Daresbury Laboratory Technical Report DL-TR-00-001, 2000.
[45] Richardson SM. Fluid mechanics. New York: Hemisphere Publishing Corp; 1989.